

# Low-Temperature Kinetic Behavior of the Bimolecular Reaction OH + HBr (76–242 K)

Dean B. Atkinson, Veronica I. Jaramillo, and Mark A. Smith\*

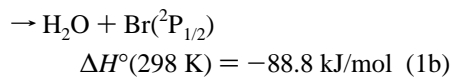
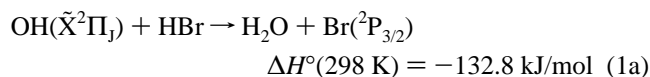
Department of Chemistry, University of Arizona, Tucson, Arizona 85721

Received: November 12, 1996; In Final Form: February 21, 1997<sup>®</sup>

The temperature dependence of the rate coefficient for the atmospherically important radical–molecule reaction OH + HBr has been investigated between 76 and 242 K using a pulsed uniform supersonic flow reactor. The current work indicates that the rate coefficient shows significant inverse temperature dependence only below 150 K. These results verify that within the terrestrial atmosphere, the OH + HBr reaction manifests a temperature-independent bimolecular rate coefficient  $k = (1.2 \pm 0.2) \times 10^{-11} \text{ cm}^3 \text{ s}^{-1}$ .

## Introduction

The reactions of atomic bromine and bromine oxide (BrO) are known to play key roles in the catalytic destruction of ozone in the terrestrial atmosphere.<sup>1</sup> The effectiveness with which a given radical destroys ozone through catalytic cycles, the rates of conversion to stable sink/reservoir species, and the regeneration of the active species determines its impact on stratospheric chemistry. The regeneration reaction



proceeds at a rate which is over an order of magnitude greater than the corresponding hydrogen chloride reaction at 300 K.<sup>1</sup> This, in combination with many other factors, has the effect of increasing the ozone depletion potential (ODP) of bromine beyond that of chlorine.<sup>2</sup>

The first determination of the temperature dependence of the rate coefficient for reaction 1 was reported by Ravishankara and co-workers in 1979.<sup>3</sup> The rate coefficient was found to be independent of temperature in the 249–416 K range. Six different temperature points in this range were averaged to provide a recommended bimolecular rate coefficient,  $k = (1.19 \pm 0.14) \times 10^{-11} \text{ cm}^3 \text{ s}^{-1}$  applicable to this temperature window. Since then several groups, including that of Ravishankara, have remeasured the rate coefficient at 298 K and find general agreement with the recommended value at this temperature.<sup>4–6</sup> Recently, Sims et al.<sup>7</sup> measured the temperature dependence of the rate coefficient into the ultralow-temperature range (23–295 K) and found a strong inverse temperature dependence. These data were fit to a simple model derived from quantum scattering calculations,<sup>8</sup> with the fit exceeding the accepted 250–300 K value by almost a factor of 2. Additionally, the ultralow-temperature behavior of this reaction has been predicted using statistical adiabatic capture theory.<sup>9</sup>

Given that the lower stratospheric temperatures relevant for OH and halocarbon chemistry extend to nearly 180 K and are routinely around 200 K, while the recommended rate behavior is based predominantly upon data obtained above 240 K, careful reexamination of the rate coefficient at low temperature is clearly necessary. We have applied a pulsed axisymmetric Laval flow technique for the generation of low-temperature environments

amenable to laboratory radical–molecule kinetic study.<sup>10</sup> Our technique is similar to the CRESU experiment of Sims et al.<sup>7</sup> in that low temperatures are achieved using the properties of a uniform supersonic expansion. Several differences exist, however, regarding radical generation, density regimes, and temperature resolution. Since both experiments are in their infancies regarding the measurement of laboratory rate coefficients for radical–molecule reactions, it is valuable to conduct complementary investigations. This stratospherically relevant reaction provides an excellent benchmark and forms the topic of this study.

## Experimental Section

**Pulsed Uniform Supersonic Expansion Flow Reactor.** A detailed description of our pulsed uniform supersonic expansion flow reactor is presented elsewhere,<sup>10</sup> and only an overview will be given here (see Figure 1). The properties of the uniform supersonic expansion flow, also known as a Laval flow, are exploited to produce a low-temperature uniform density environment, very analogous to conventional flow reactors, except with a much higher (supersonic) hydrodynamic velocity and without communication with physical walls. The flow is produced by expanding a suitable buffer gas through a converging–diverging (Laval) nozzle into a chamber with a background pressure which is tailored to prevent further radial expansion. A small predetermined amount of radial expansion during the nozzle transit causes the flow to accelerate to a particular design Mach number. Further expansion is prevented by collimation of the flow streamlines followed by injection of this flow into the pressure matched environment. Details of the nozzle design criteria are presented in a recent publication.<sup>10</sup> The consequences of fixed Mach number in the postnozzle flow include constant flow speed, density, and local temperature. The density regimes employed ( $1 \times 10^{16}$ – $5 \times 10^{17} \text{ molecules cm}^{-3}$ ) also ensure local thermal equilibrium. The extent of cooling in the gas depends on the design Mach number. To a first approximation, the isentropic relation gives the flow temperature,  $T$ , and density,  $\rho$ , relative to the preexpansion conditions:

$$\frac{T}{T_0} = \left(1 + \frac{\gamma - 1}{2} M^2\right)^{-1} \quad (2)$$

$$\frac{\rho}{\rho_0} = \left(1 + \frac{\gamma - 1}{2} M^2\right)^{-1/\gamma - 1} \quad (3)$$

where  $M$  is the Mach number, and  $\gamma$  is the heat capacity ratio  $C_p/C_v$ . A thermostated bath and recirculating system are used to control the preexpansion temperature continuously between

<sup>®</sup> Abstract published in *Advance ACS Abstracts*, April 15, 1997.

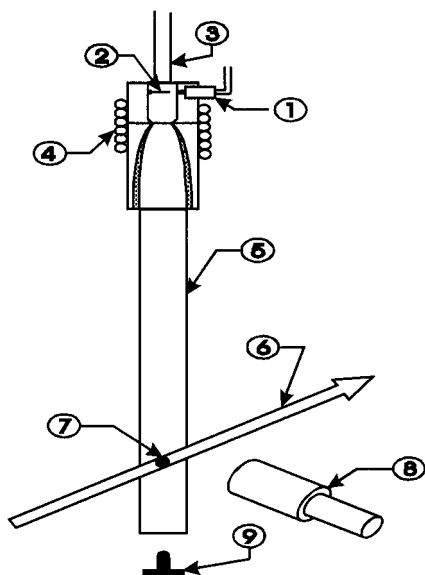


**Figure 1.** Block diagram of the pulsed uniform supersonic expansion reactor: 1, pulsed valve; 2, discharge electrode; 3, nozzle translator; 4, cooling/heating coils; 5, uniform flow; 6, LIF laser path; 7, LIF image point; 8, LIF camera; 9, impact pressure transducer.

**TABLE 1: Summary of the Results of This Study for the Reaction OH + HBr**

nozzle <sup>a</sup>	Mach <sup>b</sup> no.	stagnation temp (K)	flow temp (K)	flow density (cm <sup>-3</sup> )	<i>k</i> <sub>bimolecular</sub> (cm <sup>3</sup> /s)
M151E17	1.5	350	242	$9.6 \times 10^{16}$	$1.1(\pm 0.1) \times 10^{-11}$
M205E17	2.0	400	222	$5.4 \times 10^{17}$	$1.3(\pm 0.2) \times 10^{-11}$
M205E17	2.0	350	194	$5.2 \times 10^{17}$	$1.0(\pm 0.3) \times 10^{-11}$
M205E17	2.0	350	194	$5.2 \times 10^{17}$	$1.5(\pm 0.4) \times 10^{-11}$
M205E17	1.9	300	173	$5.2 \times 10^{17}$	$0.8(\pm 0.1) \times 10^{-11}$
M201E17	2.0	300	169	$8.7 \times 10^{16}$	$1.5(\pm 0.3) \times 10^{-11}$
M205E16	2.1	300	147	$5.1 \times 10^{16}$	$1.4(\pm 0.1) \times 10^{-11}$
M304E16	2.5	300	133	$4.5 \times 10^{16}$	$1.6(\pm 0.2) \times 10^{-11}$
M302E17	3.0	300	107	$2.0 \times 10^{17}$	$2.0(\pm 0.3) \times 10^{-11}$
M302E16	3.3	300	92	$1.5 \times 10^{16}$	$3.0(\pm 0.5) \times 10^{-11}$
M302E16	3.4	250	76	$1.9 \times 10^{16}$	$2.9(\pm 0.9) \times 10^{-11}$

<sup>a</sup> Nozzle design specification M151E17, for example, implies a design criteria of Mach 1.5 flow at an exit density of  $1 \times 10^{17}$  cm<sup>-3</sup>.

<sup>b</sup> Mach numbers are determined by OH rotational temperatures as explained above.

250 and 400 K. Using nozzles with terminal Mach numbers between 1.5 and 3.4, we are then able to access the flow temperature range 76–242 K. To cover this temperature range at a given flow density requires the use of three nozzles with different Mach numbers. To study this reaction at a variety of densities, we have employed the 11 nozzles listed in Table 1. The uniformity of the flow is verified using an impact pressure transducer, or Pitot probe, placed in the path of the flow. From the measured impact pressures,  $P_i$ , the actual Mach number can be determined using the Rayleigh–Pitot formula (eq 4). From

$$\frac{P_i}{P_0} = \left( \frac{\gamma + 1}{2} M^2 \right)^{\gamma/(\gamma-1)} \left( \frac{\gamma + 1}{2\gamma M^2 - (\gamma - 1)} \right)^{1/(\gamma-1)} \quad (4)$$

the Mach number, the flow density is determined through the use of the isentropic relationship (eq 3). In all cases the chamber pressure which gives optimum flow is found to be nearly equal to the flow pressure calculated using the ideal gas expression, providing an internal check on the system.

By flowing mixtures of a radical precursor, neutral reagent, and flow buffer and generating radicals in the preexpansion region, it is possible to conduct chemical reaction studies in the postnozzle flow at the very low temperatures extant in the

flow core. Since the expansion occurs on a time scale which permits thermal equilibration but prevents chemical equilibration (e.g., clustering and condensation), reactions can be studied at temperatures where the vapor pressure of the reagents would be prohibitively low for conventional methods. For the reaction OH + HBr, less than 1% H<sub>2</sub>O vapor, the radical precursor, and less than 2% of HBr were mixed with the nitrogen buffer, and no behavior characteristic of clustering was manifested.

**Reactant Preparation and Reaction Monitoring.** In the preexpansion subsonic region of the Laval nozzle (see Figure 1), a pulsed cold cathode discharge is used to generate OH radicals from the radical precursor, H<sub>2</sub>O, seeded into the flow. The temperature of the hydroxyl radicals is measured in the postnozzle flow using saturated LIF, exciting the S<sub>21</sub> branch of the (1,0) band of the  $\tilde{A} \leftarrow \tilde{X}$  transition, and observing the fluorescence of the (1,1) band. The radicals are found to exist only in the vibronic ground state  $\tilde{X}^2\Pi_{3/2,1/2}$  ( $v = 0$ ), indicating that complete collisional cooling occurs during the nozzle expansion. Temperatures were derived from rotational line strengths using the transition moments of Dieke and Crosswhite.<sup>11</sup> This temperature allows independent verification of the flow Mach number determined using eq 2 as well as a direct measurement of the local thermal conditions, assuming the radical has equilibrated with the buffer. This latter point has been verified by direct observation of the rotational distribution of other stable molecules (NO and HBr) seeded into the same flow conditions. In addition the observed OH rotational temperatures are found to be constant in time at even the highest density flows further supporting rotational/translational equilibrium. Both the range of the temperature discrepancies between the various methods, as well as the statistical errors in temperature from any one, typically describe an error of less than 10%. This error should be included within the temperature assignments, but also factors into the absolute density determination. This error is then an indirect contributor to the total error associated with the absolute bimolecular rate coefficient.

After the flow exits the nozzle, kinetic measurements are initiated. The radical concentration is followed using the R<sub>21</sub>-(1) and R<sub>1</sub>(1) lines of the (1,0) band of the  $\tilde{A} \leftarrow \tilde{X}$  transition, near 281 nm, under saturated absorption conditions (> 20 MW/cm<sup>2</sup>, 5 ns pulse). The relative OH concentration, as determined by fluorescence intensity is followed in flow distance. Since the flow velocity is a known constant as determined from the measured Mach number, determination of LIF probe distance directly yields the reaction time. The radical signal decay follows a simple exponential under all conditions of HBr concentration, indicating that the reaction is proceeding under pseudo-first-order conditions in HBr. Examples of this OH LIF decay is presented in Figure 2. The bimolecular rate coefficient is extracted from a plot of pseudo-first-order decay rates versus HBr density as seen in Figure 3. The eleven bimolecular rate coefficients measured between 76 and 242 K and shown in Figure 4 are the result of 76 independent rate measurements. The uncertainties reported for the bimolecular rate coefficients represent twice the standard error of the slope of the  $k_{\text{obs}}$  vs density plots. These errors are in excess of known uncertainties of all other quantities used in deriving the absolute bimolecular rate coefficients. We can identify no systematic errors in the method and feel that all significant random errors are fairly represented in the statistically derived uncertainty reported for each rate coefficient. Using nozzles with different design criteria, it is possible to determine the rate coefficient under different total pressures at a given flow temperature, allowing

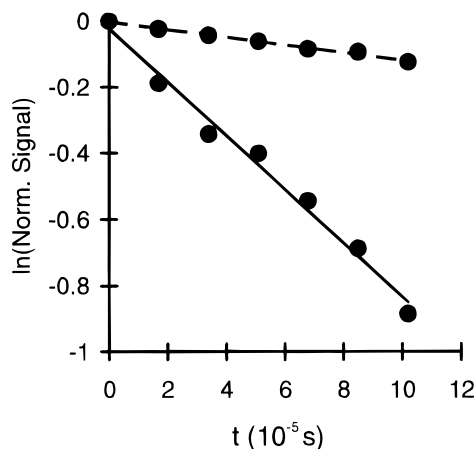


**Figure 2.** Examples of the falloff of the OH LIF signal vs reaction time for reaction 1. The reaction time was derived from the known flow velocity and the flow distance. The dashed line represents OH loss in the absence of HBr while the solid line represents loss in the presence of HBr ( $\rho_{\text{HBr}} = 3.4 \times 10^{14}$  molecules  $\text{cm}^{-3}$ ).

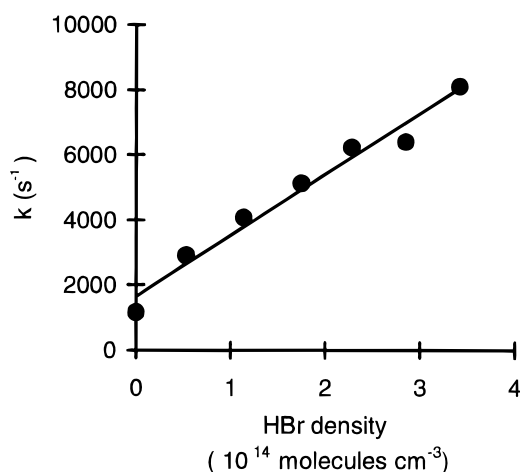


**Figure 3.** Typical pseudo-first-order rate coefficient plot vs HBr density for reaction 1. The slope represents a single temperature and flow pressure determination of the rate coefficient.

a valuable check for termolecular dependence. All results in this study indicate solely bimolecular behavior of the reactive OH loss.

The flows of the buffer, radical precursor, and reagent HBr were controlled using mass flow controllers (MKS 1159B), and the gas was introduced into the preexpansion region using two pulsed valves (General Valve Series 9) to ensure that the reagent and precursor do not interact until the last possible moment. The  $\text{N}_2$  buffer is trapped at 77 K and the radical precursor, water, is distilled to eliminate any contaminants. The HBr (Matheson-stated purity 99.8%) was freeze–thaw–degassed to remove the  $\text{H}_2$  impurity and passed through a trap at  $-40^\circ\text{C}$  to minimize the  $\text{Br}_2$  and other contaminants.<sup>3</sup> The concentration of HBr was verified by continuously monitoring the UV absorption at 220 nm, using a 10 cm path length flow cell, prior to delivery to the pulsed valve.

To verify that the HBr was not significantly destroyed by the cold cathode discharge, its concentration was independently monitored in the postnozzle Laval flow using resonantly enhanced multiphoton ionization (REMPI) and vacuum ultraviolet (VUV) absorbance. In one case, the HBr concentration was determined using rotationally resolved 2+1 REMPI via the Q branch of the (0,0) band of the  $\tilde{\text{H}}^1\Sigma^+$  intermediate state, near 251 nm in the fundamental.<sup>12</sup> An independent measure of the HBr concentration within the flow core was provided by

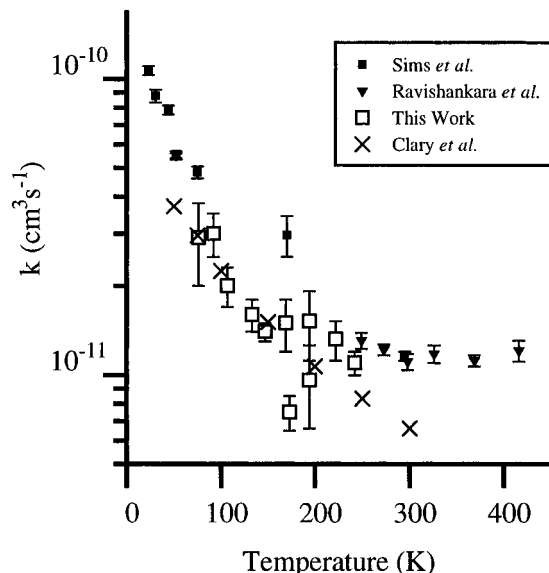


**Figure 4.** Temperature dependence of the bimolecular rate coefficient for reaction 1, including this work, the results of Sims *et al.*<sup>7</sup> and Ravishankara *et al.*<sup>3,4</sup> Also represented is the model of Clary<sup>13</sup> as explained in the text.

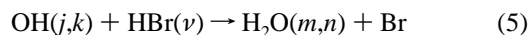
observing the VUV absorbance at 185 nm along the flow axis. The total column absorbance in the flow and stagnation region was measured with and without the discharge. Both methods indicate that greater than 95% of the HBr reactant remains unaffected by the discharge and is present at the flow temperature in the kinetic zone. Owing to the rapidity of the title reaction, small impurities generated by the discharge (e.g., H atoms) are expected to have little effect on the measured bimolecular rate coefficient.

## Results and Discussion

The results of our investigations are summarized in Table 1, along with the various flow conditions which were obtained. All of the temperature-dependence data, including this work, the results of Sims *et al.*,<sup>7</sup> and of Ravishankara *et al.*,<sup>3,4</sup> are shown in Figure 4; results of the model of Clary *et al.*<sup>8</sup> are also represented. The inverse temperature dependence of the reaction below 200 K is clear, but the onset of this dependence is more gradual than reported earlier.<sup>7</sup> Owing to the very recent and novel developments in low-temperature kinetic methodology, we cannot yet comment on the differences in results obtained in this work relative to those reported by Sims *et al.* also employing an axisymmetric supersonic flow. It is important to note, however, that the 300 K rate coefficient reported by Sims *et al.* was obtained using a nonsupersonic flow technique analogous to standard slow-flow methods. As such, the excellent comparison of this rate with the data of Ravishankara *et al.* is not surprising and does not necessarily address the accuracy of the data obtained in the supersonic flows. The invariance of the rate coefficient over greater than an order of magnitude change in total pressure in our studies indicates that this reaction manifests entirely bimolecular behavior at these temperatures, which is in line with the observations of Sims *et al.*

The model for the temperature dependence of the rate coefficient proposed by Clary<sup>8</sup> provides a good fit of the combined data of Ravishankara and this report, while importing only a small deviation from the data of Sims *et al.* (Figure 2). This model, which was derived from quantum scattering calculations, provides the first theoretical attempt to describe the temperature dependence of the rate coefficient. These

calculations were based on the rotating bond approximation (RBA).<sup>13</sup> Clary considered the



reaction, where  $j$  is the rotational state of OH,  $\nu$  is the vibrational state of HBr, while  $m$  and  $n$  are the bending mode and a local stretching mode of H<sub>2</sub>O. The potential energy surface used in this calculation was based on an accurate H<sub>2</sub>O potential and on the transition state for the OH + HCl reaction found from a quasiclassical trajectory calculation. The rate constant was calculated from Maxwell–Boltzmann averaging over the cross sections and the product with the initial velocity and then over all  $j$  values. This gives the following rate coefficient:

$$k(T) = \frac{k_0(T)(1 + 2 \sum_{j=1} \exp(-E_j/k_b T))}{\sum_{j=0} (2j+1) \exp(-E_j/k_b T)} = k_0(T) \sqrt{\frac{B\pi}{k_b T}} \quad (6)$$

where  $k_0(T)$  is the rate coefficient for OH( $j=0$ ),  $B$  is the rotational constant of OH, and  $k_b$  is the Boltzmann constant. The dominant  $T^{-1/2}$  dependence of the model is a consequence of both the strong long-range dipole–dipole interaction potential and a  $(2J+1)^{-1}$  dependence in the reactive cross section, which causes OH rotational excitation to inhibit the reaction.

There may exist a much better fitting model to explain the full range of the temperature dependence of the rate coefficient. For lower temperatures, statistical adiabatic capture theory<sup>14</sup> seems to provide an upper limit to the experimental rate constant since it assumes only a dipole–dipole interaction potential as well as allows for the open-shell nature of the OH radical. One should not overemphasize the relationship between fitting models and reaction mechanisms. The results of Clary et al. are providing the first insight into the importance of both dipolar interactions and rotational energy dependence of this reaction system. It remains unclear as to the importance of competition between direct and collision complex mediated reaction in this system, as well as the subtleties of the energy dependences of both complex formation and complex dynamics.

The results indicate that there may be a strong reaction mechanism switching that is observed at temperatures below 150 K. One possibility for this switching would be the onset of molecular association to form the HOHBr complex. Sims et al. report that at 52 K a 2-fold change in buffer density gave no rate change, consistent with a bimolecular reaction. At the higher temperatures for our study, changes in total density of greater than an order of magnitude also indicate bimolecular behavior, though the contribution of termolecular processes would be expected to be much greater in the temperature window of the Sims study.

It is important to note that the vast majority of radical–molecule reaction rate studies involve measurement only of reactant loss. The same is true for all of the data in Figure 2. It would be most helpful in resolving questions surrounding origins of strongly temperature-dependent rates and mechanism switching if molecular products were also quantitatively identified in the complete temperature window.

## Conclusion and Impact on Stratospheric Modeling

The rate coefficient of the reaction OH + HBr has been investigated in the intermediate low-temperature region (76–242 K). The reaction of hydroxyl radicals with HBr is very fast with respect to the analogous hydrogen chloride reaction (OH + HCl,  $k = 8 \times 10^{-13} \text{ cm}^3 \text{ s}^{-1}$  at 300 K, with a positive temperature dependence),<sup>1</sup> meaning that the conversion of the bromine sink/reservoir to active species will keep the relative concentration of active bromine radicals high within the terrestrial stratosphere. This has been assumed in stratospheric modeling calculations for some time, and the current results do not indicate that a major refinement of the temperature dependence of the rate coefficient is necessary. The rate coefficient had been considered to be temperature independent over the stratospherically relevant range<sup>1</sup> ( $T \geq 150 \text{ K}$ ), and this appears to be mostly valid; the rate coefficient increases by less than 10% in the range 300–180 K.

At a fundamental level, it is interesting that the dynamics of such a simple reaction should show such a rich temperature dependence. Some mechanism change appears to be occurring at low temperature, but its nature is as yet unclear. Elucidation of the mechanism active at the low temperatures would certainly be aided by product detection, and efforts are underway in our laboratory to accomplish such characterization. The reaction also remains a useful challenge to high-level dynamical theory because of the interesting rate complexity, as well as the relative simplicity regarding the number of atoms. As such, the reaction will most likely continue for a while as a benchmark for temperature-dependent elementary radical–molecule reactions.

**Acknowledgment** is made to the donors of The Petroleum Research Fund, administered by the American Chemical Society, for the partial support of this research. In addition we acknowledge the generous support of this work by the National Science Foundation under Grants CHE-8920480 and CHE-9220399 as well as the Vice President for Research at the University of Arizona. Finally, the authors wish to acknowledge helpful conversations with A. R. Ravishankara.

## References and Notes

- (1) DeMore, W. B.; Sander, S. P.; Golden, D. M.; Molina, M. J.; Hampson, R. F.; Kurylo, M. J.; Howard, C. J.; Ravishankara, A. R. *Chemical Kinetics and Photochemical Data for Use in Stratospheric Modeling, Evaluation Number 9*; JPL Publication 90–1, 1990.
- (2) Wayne, R. P. *Chemistry of Atmospheres*, 2nd ed.; Oxford University Press: New York, 1993; p 165.
- (3) Ravishankara, A. R.; Wine, P. H.; Langford, A. O. *Chem. Phys. Lett.* **1979**, *63*, 479.
- (4) Ravishankara, A. R.; Wine, P. H.; Wells, J. R. *J. Chem. Phys.* **1985**, *83*, 447.
- (5) Cannon, B. D.; Robertshaw, J. S.; Smith, I. W. M.; Williams, M. D. *Chem. Phys. Lett.* **1984**, *105*, 380.
- (6) Jourdain, J. L.; Le Bras, G.; Combourieu, J. *Chem. Phys. Lett.* **1981**, *78*, 483.
- (7) Sims, I. R.; Smith, I. W. M.; Clary, D. C.; Bocherel, P.; Rowe, B. R. *J. Chem. Phys.* **1994**, *101*, 1748.
- (8) Clary, D. C.; Nyman, G.; Hernandez, R. *J. Chem. Phys.* **1994**, *101*, 3704.
- (9) Clary, D. C.; Nyman, G.; Hernandez, R. *J. Chem. Soc. Faraday Trans.* **1993**, *89*, 2185.
- (10) Atkinson, D. B.; Smith, M. A. *Rev. Sci. Instrum.* **1995**, *66*, 4434.
- (11) Dieke, G. H.; Crosswhite, H. M. *J. Quant. Spectrosc. Radiat. Transfer* **1962**, *2*, 97.
- (12) Callaghan, R.; Gordon, R. J. *J. Chem. Phys.* **1990**, *93*, 4624.
- (13) Clary, D. C. *J. Chem. Phys.* **1991**, *95*, 7298.
- (14) Clary, D. C.; Nyman, G.; Hernandez, R. *J. Chem. Soc., Faraday Trans.* **1993**, *89*, 2185.